

Task Specific Pruning with LLM-Sieve: How Many Parameters Does Your Task Really Need?

Waleed Reda

Microsoft Research

waleedreda@microsoft.com

Abhinav Jangda

Microsoft Research

ajangda@microsoft.com

Krishna Chintalapudi

Microsoft Research

krchinta@microsoft.com

Abstract

As Large Language Models (LLMs) are increasingly being adopted for narrow tasks—such as medical question answering or sentiment analysis—and deployed in resource-constrained settings, a key question arises: how many parameters does a task actually need? In this work, we present LLM-Sieve, the first comprehensive framework for task-specific pruning of LLMs that achieves 20–75% parameter reduction with only 1–5% accuracy degradation across diverse domains. Unlike prior methods that apply uniform pruning or rely on low-rank approximations of weight matrices or inputs in isolation, LLM-Sieve (i) learns task-aware joint projections to better approximate output behavior, and (ii) employs a Genetic Algorithm to discover differentiated pruning levels for each matrix. LLM-Sieve is fully compatible with LoRA fine-tuning and quantization, and uniquely demonstrates strong generalization across datasets within the same task domain. Together, these results establish a practical and robust mechanism to generate smaller performant task-specific models.

1 Introduction

Large Language Models (LLMs) are increasingly employed for domain-specific tasks and deployed in environments with limited computational and memory resources, such as personal devices. When an LLM—such as LLaMA 3.1—is used for a narrow task (e.g., medical question answering or sentiment analysis), it is reasonable to hypothesize that only a fraction of its parameters are necessary. This follows from the observation that the distribution of inputs, outputs, and the reasoning complexity required for a specialized task typically constitutes a strict subset of what the full model was trained to handle. Consequently, it should be possible to identify and remove parameters that are redundant or irrelevant for the task, thereby reducing the model’s memory footprint and inference latency. In this work, we investigate the central question: *Given a specific downstream task, what fraction of an LLM’s parameters can be pruned with minimal or no loss in performance—and how can such pruning be achieved effectively?*

While pruning has been extensively studied in neural networks [1], the question of how many parameters are truly needed for a specific task remains open for LLMs. We address this with LLM-Sieve, a task-aware pruning framework that reveals substantial redundancy in large models. We find that 25–75% of parameters can be removed with only 1–5% drop in task accuracy, depending on the model and task—yielding significant gains in memory and inference efficiency. In contrast, existing methods typically achieve only 1–5% reduction in parameters under similar constraints. To our knowledge, this work is the first to expose such large redundancies in LLM parameters for narrow tasks, enabling more efficient task specialization.

State-of-the-art pruning methods often rely on low-rank approximations to reduce the dimensionality of matrix multiplications in LLMs, based on the intuition that most relevant information lies in a lower-dimensional subspace [2, 3, 4]. These methods typically project either the weight matrices or

the input distributions independently, assuming an implicit alignment between their subspaces—a condition that may not hold in practice. In contrast, LLM-Sieve learns a joint projection that directly approximates the final output, better capturing task-specific structure.

Second, LLM-Sieve introduces differentiated pruning, in which each matrix in the LLM is pruned to a task-dependent degree. Existing approaches typically apply uniform pruning ratios across all layers and matrix types—often leaving pruning granularity as a manual hyperparameter. In contrast, LLM-Sieve employs a Genetic Algorithm (GA) to automatically explore optimal, non-uniform pruning configurations. Our GA search revealed that not all matrices contribute equally to performance: some can be pruned by up to 95% with minimal loss, while others, identified as *bottleneck matrices*, exhibit significant degradation even with modest pruning (e.g., 5%).

To compensate for pruning-induced degradation, many existing approaches apply Low-Rank Adaptation (LoRA) [4] to recover task performance. However, we observe that state-of-the-art pruning methods often over-rely on LoRA, resulting in dataset-specific tuning that harms generalization across unseen datasets within the same task domain. In contrast, LLM-Sieve pruned models exhibit strong task domain generalization. We also find that LLM-Sieve and LoRA are in fact complementary—applying LoRA after pruning yields smaller, fine-tuned models with strong performance. Moreover, compression techniques such as quantization can be applied after pruning to further reduce model size. These results suggest a practical deployment pipeline with pruning, fine-tuning, and quantization, to obtain compact, efficient, and robust task-specific LLMs.

In summary, our contributions are:

- We propose LLM-Sieve, a novel task-specific pruning technique that removes 25–75% of an LLM’s parameters with only 1–5% accuracy loss—vastly outperforming prior methods and resulting in commensurate gains in memory efficiency and inference latency. To our knowledge, it is the first framework to reveal such large redundancy in LLM parameters and systematically address how much of an LLM is truly needed for narrow tasks.
- LLM-Sieve introduces two key techniques: (i) it learns low-rank projections that accurately capture task-specific low-rank subspaces for each matrix multiplication in the LLM, and (ii) it applies differentiated pruning via a Genetic Algorithm, showing that some matrices can be pruned by up to 95% with minimal accuracy loss, while others—*bottleneck matrices*—degrade sharply with even minor pruning. We believe identifying such task-critical components may offer insight into how knowledge and reasoning are organized within LLMs.
- We show that LLM-Sieve is compatible with LoRA fine-tuning and quantization, and generalizes well to unseen datasets within the same task domain. In contrast, prior methods often overfit to the calibration set, relying heavily on LoRA and failing to generalize across datasets.

2 Related Work

Recent advancements in compressing large language models (LLMs) have led to various techniques aimed at reducing model size and computational requirements while maintaining performance. These methods can be broadly categorized into either pruning strategies or other downsizing approaches such as quantization and knowledge distillation.

Pruning Techniques. Pruning methods can be classified into unstructured and structured approaches. Unstructured pruning typically removes weights based on magnitude [5, 6], resulting in sparse matrices. While effective at reducing parameter count, such sparsity often yields little practical speedup on GPUs, which are not optimized for irregular memory access patterns [7]. Unstructured pruning techniques like SparseGPT [7] and Wanda [8] often use light-weight tuning to recover performance after aggressive pruning.

Structured pruning, on the other hand, removes entire attention heads, neurons, or matrix blocks, yielding dense submatrices that better align with GPU hardware. LLM-Pruner [9], for example, leverages gradient-based saliency to identify and remove less critical coupled structures within the model, such as neuron channels and attention heads.

Among structured methods, low-rank approximation [10] offers a particularly efficient path by reducing the dimensions of matrix multiplications. SliceGPT [2] reduces model size by projecting inputs and intermediate activations into lower-dimensional subspaces, effectively pruning entire

rows or columns from weight matrices. LASER [3] focuses on approximating weight matrices themselves through selective low-rank decompositions, targeting specific layers within the transformer architecture. LLM-Sieve builds on this structured, low-rank perspective, but departs from prior approaches by learning a joint projection over both inputs and outputs, providing higher fidelity.

Other LLM Downsizing Techniques. Beyond pruning, quantization and knowledge distillation are widely used to reduce LLM size. Quantization [11, 12, 13, 14] lowers precision (e.g., from FP32 to INT8/FP4), reducing memory and compute with minimal accuracy loss [15, 16]. Distillation [17] transfers knowledge from a larger teacher model to a smaller student by aligning outputs. These techniques are orthogonal to pruning and can be used in combination.

3 Transformer Architecture Background

In this section, we provide the necessary background on transformer networks [18], required for the rest of the paper. The transformer architecture (Figure 1) comprises a series of layers, each composed of a multi-head self-attention mechanism followed by a feed-forward network (FFN) block. Between these blocks, normalization layers such as LayerNorm [19] or RMSNorm [20] are applied, often in conjunction with residual connections.

Inference begins with an embedding layer that transforms input token IDs and position IDs into dense vectors. After embeddings, the signal matrix $X \in \mathbb{R}^{N \times D}$, where D denotes the embedding dimension and N the sequence length, is passed through a LayerNorm operation which normalizes each row of X . After this X is transformed as it passes through in each of the layers.

In the attention block at the k^{th} layer, the signal is projected into key ($K^k = XW_K^k$), query ($Q^k = XW_Q^k$), and value ($V^k = XW_V^k$) matrices using respective weight matrices W_K^k , W_Q^k , and W_V^k , usually concatenated into a single matrix W_{QKV}^k for efficient computation. The self-attention mechanism computes the attention scores:

$$\text{Attention}(Q^k, K^k, V^k) = \text{softmax}\left(\frac{Q^k(K^k)^T}{\sqrt{D}}\right)V^k \quad (1)$$

Multi-head attention extends this by performing these operations in parallel across h heads, concatenating their outputs, and applying a final projection:

$$\text{MultiHead}(Q^k, K^k, V^k) = \text{Concat}(\text{head}_1, \text{head}_2, \dots, \text{head}_h)W_O^k \quad (2)$$

where W_O^k is called the output projection matrix.

The FFN block typically consists of two linear transformations separated by a non-linear activation function, such as ReLU or GeLU. The operation of an FFN block is given by:

$$\text{FFN}(X) = \sigma(XW_1^k + b_1^k)W_2^k + b_2^k \quad (3)$$

where W_1^k and W_2^k are weight matrices, b_1^k and b_2^k are biases, and σ represents the activation function.

These blocks are repeated in every layer, and the embedding output has to pass through all the layers. Due to the autoregressive nature of transformers, outputs are fed back and multiple forward passes are required to produce the output to the prompt.

4 LLM-Sieve

LLM-Sieve aims to reduce the number of parameters in a Large Language Model (LLM) while ensuring that the degradation in end-to-end task performance remains within a user-specified tolerance ϵ . Let $L(\Theta)$ denote the original LLM with parameters Θ , which maps an input set \mathbf{X} to outputs $\mathbf{Y} = L(\mathbf{X} | \Theta)$. A task-specific evaluation function $e(\mathbf{Y})$ quantifies the quality of the model’s outputs—this may be a standard metric such as F1 score or a learned quality score, e.g., from GPT-4o. The objective of LLM-Sieve is to construct a pruned model $\hat{L}(\hat{\Theta})$ such that its performance on a task-specific dataset \mathbf{X}_C satisfies: $e(\hat{L}(\mathbf{X}_C | \hat{\Theta})) \geq a_0$, where a_0 is the target performance level, defined in relation to the original model’s performance $a^* = e(L(\mathbf{X}_C | \Theta))$ as: $\frac{a^* - a_0}{a^*} = \epsilon$. In other words, LLM-Sieve ensures that the pruned model maintains at least $(1 - \epsilon)$ of the original model’s task-specific performance.

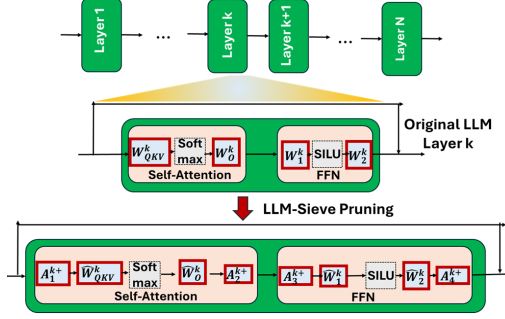


Figure 1: How each matrix multiplication in an LLM is approximated in LLM-Sieve.

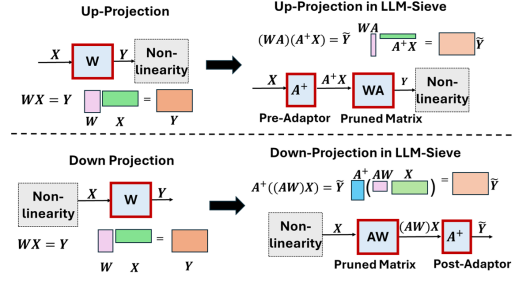


Figure 2: Low-rank approximate multiplications in LLM-Sieve pruning.

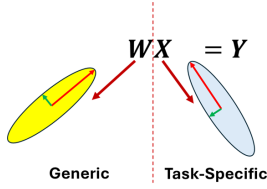


Figure 3: Intuition behind pruning in LLM-Sieve.

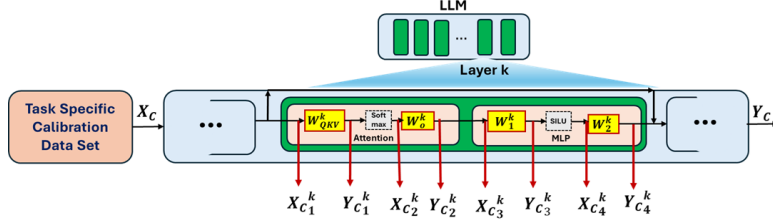


Figure 4: Calibration step in LLM-Sieve

4.1 LLM-Sieve Pruning

LLM-Sieve approximates each matrix multiplication in a task-specific lower-dimensional subspace (Figure 1). To preserve the dimensionality required by surrounding non-linear transformations, it applies different approximation strategies to the matrix multiplications that precede and follow non-linear layers.

Approximating Pre-Nonlinear Multiplications (Figure 2). In these multiplications, $Y = WX$, where $W \in \mathbb{R}^{H \times D}$ is the weight matrix with output dimension H and input dimension D , and $Y \in \mathbb{R}^H$ serves as input to a non-linear layer. For example W_{QKV} in self-attention layer, followed by Softmax and W_1 in the FFN, followed by ReLU/Gelu. These multiplications are approximated as,

$$\tilde{Y} = (WA)(A^\dagger X) \quad (4)$$

where, A^\dagger is the pseudo-inverse of the adaptor matrix $A \in \mathbb{R}^{R \times H}$ and $R < D$ is the reduced rank of $\tilde{W} = WA \in \mathbb{R}^{R \times H}$. During inference, inputs are first transformed into a low-rank space as $\hat{X} = A^\dagger X \in \mathbb{R}^R$ and then the outputs are computed as $\tilde{Y} = \tilde{W}\hat{X} \in \mathbb{R}^H$.

Approximating Post-Nonlinear Multiplications (Figure 2). In these multiplications, $Y = WX$, $W \in \mathbb{R}^{D \times H}$, the input X is the output of a non-linear layer. For example W_o in self-attention, preceded by Softmax and W_2 in the FFN, preceded by ReLU/Gelu. These multiplications are approximated as,

$$\tilde{Y} = A^\dagger ((AW)X) \quad (5)$$

where, A^\dagger is the pseudo-inverse of the adaptor matrix $A \in \mathbb{R}^{R \times D}$ and $R < D$ is the reduced rank of $\tilde{W} = AW \in \mathbb{R}^{R \times H}$. During inference, the outputs are computed in a low dimensional space as $\hat{Y} = \tilde{W}X \in \mathbb{R}^R$ and then projected up using $\tilde{Y} = A^\dagger \hat{Y} \in \mathbb{R}^D$.

Intuition into LLM-Sieve's Low Rank Projections. In any matrix multiplication $Y = WX$ within an LLM, the inputs X depend on the task-specific data distribution, whereas the weight matrices W are task-agnostic and trained for general-purpose language modeling. Existing pruning methods typically fall into two categories. The first reduces matrix dimensionality using Singular Value Decomposition (SVD), but this approach does not exploit the limited support of the task-specific input distribution. The second performs Principal Component Analysis (PCA) on the inputs X to identify a low-rank projection, assuming that input compression alone suffices. However, as illustrated in Figure 3, the subspaces spanned by W and X are not necessarily aligned, which limits

the effectiveness of such decompositions. Rather than projecting weights or inputs independently, LLM-Sieve learns task-specific projections by directly approximating the output \mathbf{Y} . Specifically, it seeks projections that minimize the average reconstruction error: $\|\mathbf{Y} - \tilde{\mathbf{Y}}\|$.

LLM-Sieve Calibration Step. The first step in LLM-Sieve is to perform inference over all inputs in the task-specific calibration data set \mathbf{X}_C , capturing input-output pairs for every matrix multiplication in the LLM (Figure 4). For instance, Llama-3.1-70B has 320 matrix multiplications – each of its 80 layers contains four key multiplications: $\mathbf{W}_{QKV}, \mathbf{W}_o, \mathbf{W}_1$ and \mathbf{W}_2 . Thus, for Llama-3.1-70B, 320 input-output pairs are captured, where each layer ($k = 1, \dots, 80$) contributes $\langle \mathbf{X}_{C_1}^k, \mathbf{Y}_{C_1}^k \rangle, \langle \mathbf{X}_{C_2}^k, \mathbf{Y}_{C_2}^k \rangle, \langle \mathbf{X}_{C_3}^k, \mathbf{Y}_{C_3}^k \rangle, \langle \mathbf{X}_{C_4}^k, \mathbf{Y}_{C_4}^k \rangle$ corresponding to the four multiplications per layer. These measurements serve to find the optimal values of the adaptor matrices \mathbf{A}_i^k as described next.

Finding Adaptors \mathbf{A}_i^k . For each matrix multiplication in layer k , LLM-Sieve learns a task-specific adaptor matrix \mathbf{A}_i^k by solving a regression problem that minimizes the reconstruction error between the true outputs over the calibration data set $\mathbf{Y}_{C_i}^k$ and its low-rank approximation $\tilde{\mathbf{Y}}_{C_i}^k$. \mathbf{A}_i^k is determined by a gradient decent to minimize: $\|\mathbf{Y}_{C_i}^k - \tilde{\mathbf{Y}}_{C_i}^k\|$.

Pruning Factor. Since, H and D are fixed in each multiplication, the choice of R determines the extent of pruning. After pruning, the model stores $\hat{\mathbf{W}}$ instead of \mathbf{W} along with the adaptor \mathbf{A} . Thus, the total parameters after pruning are $R(H + D)$. The *pruning factor* then is given by $p = \frac{R(H+D)}{DH}$.

4.2 Differentiated Pruning

LLM-Sieve pruning, as described in Section 4.1, requires specifying a parameter R that defines the intermediate rank used in each adaptor matrix \mathbf{A} . In a model with N layers, there are $4N$ matrix multiplications—corresponding to $\mathbf{W}_{QKV}, \mathbf{W}_o, \mathbf{W}_1$, and \mathbf{W}_2 in each layer. Crucially, each of these multiplications may vary in its sensitivity to pruning, as different matrices encode differing amounts of task-specific information. To support differentiated pruning, we define the pruning factor vector: $\mathbf{p} = \langle p_1^1, p_2^1, \dots, p_4^N \rangle \in \mathbb{R}^{4N}$, where each $p_i^k \in [0, 1]$ specifies the fraction of parameters retained in the i -th matrix of layer k .

Recall that the objective of LLM-Sieve is to minimize the total parameter count while ensuring that the loss in end-to-end task performance does not exceed a tolerance ϵ . Therefore, the goal of differentiated pruning is to determine the optimal pruning factor vector \mathbf{p} that satisfies:

$$\min_{\mathbf{p}} \quad \|\hat{\Theta}(\mathbf{p})\|_0 \text{ subject to } \frac{a^* - e(\hat{L}(\mathbf{X}_C | \hat{\Theta}(\mathbf{p})))}{a^*} \leq \epsilon, \quad (6)$$

where $\hat{\Theta}(\mathbf{p})$ denotes the pruned parameter set induced by \mathbf{p} , and a^* is the baseline performance of the unpruned model. The end-to-end evaluation function $e(\hat{L}(\mathbf{X}_C | \hat{\Theta}(\mathbf{p})))$ may not be differentiable—for example being defined as an average quality score obtained from a black-box model such as GPT-4o. This non-differentiability precludes using gradient-based optimization for finding \mathbf{p} .

4.2.1 Common Approach: Uniform Pruning (UP)

A commonly employed approach in many pruning techniques is to prune each matrix by the same pruning factor p^* . This constraint vastly reduces the search space and practitioners typically determine a suitable value of p^* through trial and error.

Uniform Ratio Pruning With Binary Search. To automate the selection of an optimal uniform pruning factor p^* , LLM-Sieve employs a binary search strategy. The goal is to identify the smallest value of p^* (greatest pruning) such that the pruned model still satisfies the end-to-end performance constraint. At each iteration, we maintain an upper bound p_{up} and a lower bound p_{low} such that the performance constraint (i.e., degradation $< \epsilon$) is violated at p_{low} but satisfied at p_{up} .

We evaluate model performance on the calibration dataset using the midpoint pruning ratio: $\frac{p_{\text{up}} + p_{\text{low}}}{2}$. If the pruned model with ratio p_{mid} meets the accuracy constraint, we update the upper bound: $p_{\text{up}} \leftarrow p_{\text{mid}}$. Otherwise, we update the lower bound: $p_{\text{low}} \leftarrow p_{\text{mid}}$. This process repeats until convergence to the optimal pruning factor p^* .

4.2.2 Differentiated Pruning With Genetic Algorithm

Unlike uniform pruning, which optimizes a single global pruning factor, differentiated pruning requires navigating a high-dimensional, non-convex, and non-differentiable search space—making gradient-based or exhaustive search methods impractical; consequently we use a Genetic Algorithm (GA) for efficient exploration.

A Genetic Algorithm (GA) is an evolutionary optimization technique inspired by natural selection that is often employed to efficiently navigate the combinatorial search spaces. A population of chromosomes, each chromosome encoding a particular point in the search space, is maintained. The population evolves over successive generations through biologically inspired operations: crossover (which combines segments of two parent chromosomes) and mutation (which introduces small random changes). After each generation, only the fittest individuals—those with pruning configurations yielding the highest task-specific performance—are retained, ensuring gradual convergence toward an optimal or near-optimal solution.

Chromosome Encoding in LLM-Sieve. In our GA, each chromosome is simply the pruning vector. In each generation, a population of p chromosomes $\mathbf{P} = [\mathbf{p}_1, \mathbf{p}_2, \dots, \mathbf{p}_M]$ is maintained (we chose $M = 100$). At the beginning, an initial set population of chromosomes is initialized by picking pruning factors randomly from a predefined sub-set of values in $(0, 1) - \{1, 0.9, 0.75, 0.6, 0.5, 0.35, 0.25, 0.2, 0.1, 0.05\}$ in our implementation. 10 of the chromosomes are also initialized with all pruning factors set to the same value.

Crossover Operation. In each crossover operation, two chromosomes are picked with probability proportional to their fitness functions. A random split point is selected, and the chromosomes are severed at this position. The offspring chromosomes are then formed by swapping and recombining the left and right segments. We set the crossover probability to 0.5 in our implementation.

Mutation Operation. The mutation operator randomly perturbs the chromosome by increasing or decreasing reduction factors by one step from the sub-set of predefined values at random locations. Mutation probability is kept at 0.2% in our implementation.

End-to-end Fitness Function. The fitness function is central to guiding the GA’s search. Since LLM-Sieve aims to maximize pruning while maintaining accuracy above a target threshold a_0 , the fitness function is designed to reward compression when performance exceeds a_0 and penalize it exponentially when it falls below:

$$F(\mathbf{r}, a) = c(\mathbf{r}) \times \left(1 + e^{50(a - a_0)}\right) \quad (7)$$

Here, $c(\mathbf{r})$ denotes the ratio of parameters in the pruned model to that of the original, and a is the measured end-to-end task accuracy. As described in our evaluation setup, we use GPT-4o-as-judge to score performance on our task dataset. The Genetic Algorithm terminates when no significant improvement (defined as less than 5% change) is observed over 10 consecutive generations.

Embarrassingly Parallel Implementation To improve the efficiency of running the GA, we precompute pruned matrices for a fixed set of pruning factors. As these computations are independent, they can be performed in parallel. The GA initializes and mutates chromosomes by selecting from this precomputed set. During fitness evaluation, each chromosome is used to instantiate a separate LLM with the corresponding matrices, enabling parallel evaluation of candidate solutions.

5 Evaluation

We evaluate LLM-Sieve on three models of varying sizes—Phi-3-mini (3.8B), LLaMA-3.1 (8B), and LLaMA-3.1 (70B)—across three tasks: **i) Generic RAG** and **ii) Medical RAG**, both of which involve answering a question using provided context passages, and **iii) Sentiment Analysis**, which involves classifying a given text as having either positive or negative sentiment. In all cases, the model’s predicted output is compared against a reference answer for evaluation.

Datasets. For each task we use two different well known popular public datasets. For Generic RAG, we use *HotpotQA* [21] (*Gen RAG-I*) and *NaturalQA* [22] (*Gen RAG-II*). For Medical RAG, we use *PubMedQA* [23] (*Med RAG-I*) and *MedMCQA* [24] (*Med RAG-II*). For Sentiment Analysis we use *IMDB* [25] (*Sentiment-I*) and *SST2* [26] (*Sentiment-II*).

Performance – Accuracy Measurement. We use GPT-4o-as-a-judge [27] to measure one-shot task accuracy since it is known to be a more robust approach than commonly used metrics like Exact

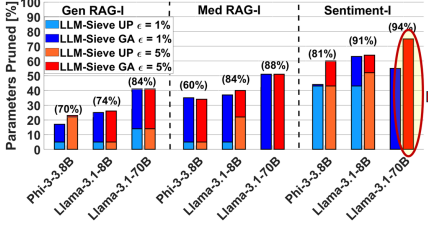


Figure 5: Pruning performance of LLM-Sieve for different models and tasks. On the right, the layer-wise fraction of parameters retained for Llama-3.1-70B on Sentiment-I shows a clear pattern.

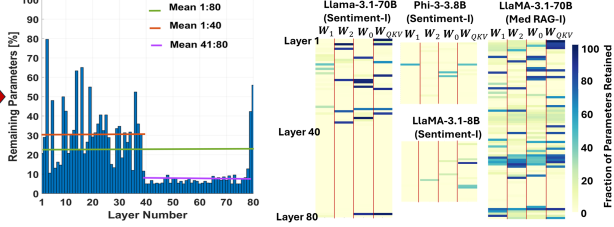


Figure 6: The fraction of parameters retained in each matrix of various models. (more details in A.4).

Match, Quasi-Exact Match, and F1 [28]. To evaluate each prompt, GPT-4o is instructed in the query to judge each answer as either “correct” or “incorrect” by comparing the response answer to the ground-truth. The accuracy is measured as:

$$\text{Accuracy} = \frac{\text{Number of correct answers}}{\text{Number of prompts}}$$

Calibration Datasets. For each task, calibration data was generated by randomly sampling prompts to total 200K tokens from Gen RAG-I, Med RAG-I and Sentiment-I. We use only 200k since our sensitivity analyses indicated that larger calibration datasets do not provide additional benefits (see Appendix A.1). *Note that we do not use Gen RAG-II, Med RAG-II, or Sentiment-II as calibration datasets, as our goal is to use them to evaluate cross-dataset generalization performance.*

State-of-the-Art Comparisons. We compare **LLM-Sieve-GA** (differentiated pruning using a Genetic Algorithm) and **LLM-Sieve-UP** (uniform pruning using binary search) against the three best performing techniques we found. **LASER** [3] employs Singular Value Decomposition (SVD) to derive low-rank approximations of weights while **SliceGPT** [2] applies low-rank projections to input representations. **LLM-Pruner** [9], in contrast, uses gradient-based structural pruning to remove less important parameter groups. Both LLM-Pruner and SliceGPT use calibration data, and we replace their default datasets with our own task datasets.

Platform Setup. LLM-Sieve is implemented on VLLM [29] for improved memory efficiency and scalable inference. Experiments run on 96 A100 GPUs across 12 VMs. To scale pruning, we enable pipeline parallelism but disable tensor parallelism, as it requires increased synchronization for collecting input-output pairs of each matrix.

5.1 How many parameters can LLM-Sieve remove?

Figure 5 reports the percentage reduction in model size across three models and three datasets, for two tolerance thresholds $\epsilon = 1\%$ (orange/red) and $\epsilon = 5\%$ (blue). The baseline accuracy of the original uncompressed model is noted in parentheses. Since the performance of the Genetic Algorithm (GA)-based pruning is strictly superior to uniform pruning, the figure stacks their contributions to highlight the differential gain. *The total reduction can be substantial—ranging from 20% to 75% depending on the model size, narrowness of the task (based on its input/output space and reasoning complexity), and tolerated performance degradation.* Larger models and narrower tasks (e.g., sentiment analysis) tend to exhibit greater extent of pruning. For instance, the LLaMA-3.1-70B model on the Sentiment-I task—which only requires a binary true/false output—can be pruned by up to 75%.

How Much Does Differentiated Pruning Help—and Why? Figure 5 shows that differentiated pruning consistently removes an additional 10–50% of the total parameters beyond what uniform achieves, as indicated by the dominant contribution of the dark red/blue regions. In the case of LLaMA-3.1-70B on Sentiment-I, the majority of the 75% reduction is due to differentiated pruning, while uniform contributes $< 5\%$. To understand this disparity, Figure 5 also shows the fraction of parameters retained per layer. Strikingly, layers 41–79 (the latter half of the model) retain less than 10% of their parameters on average, whereas layers 1–40 preserve over 30%. Some layers, including the first and last, retain as much as 70–80%, illustrating the uneven importance of different layers.

Bottleneck Matrices. Figure 6 (more details in Appendix sec. A.4) presents a layer-by-layer and matrix-by-matrix heatmap of parameter retention for each matrix type for Sentiment-I across all three models as well as Llama-3.1-70B for Med RAG-I. Dark blue cells denote matrices that were retained almost entirely—these are the so-called *bottleneck matrices*. In LLaMA-3.1-70B for Sentiment-I and

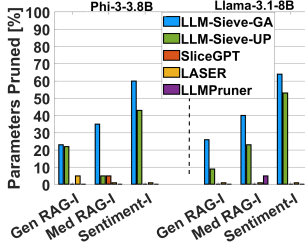


Figure 7: LLM-Sieve compared to state-of-the-art pruning techniques.

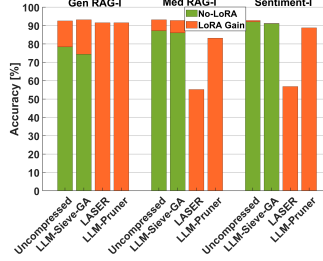


Figure 8: Effect of LoRA fine-tuning on for Llama-3.1-8B.

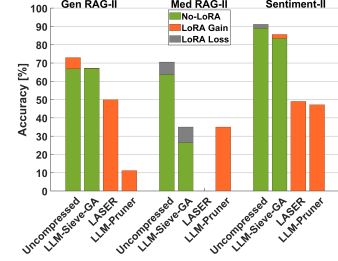


Figure 9: Effect of LoRA fine-tuning on unseen datasets for LLaMA-3.1 8B.

Med RAG-I, several matrices such as W_{QKV} in the first and last few attention layers resist pruning. The presence of bottleneck matrices limits the effectiveness of uniform pruning, as it applies global thresholds indiscriminately across all matrices. In contrast, differentiated pruning can circumvent the bottlenecks by effectively "pruning around" the bottlenecks.

5.2 How does LLM-Sieve compare to the state-of-the-art?

As shown in Figure 7, both LLM-Sieve-GA and LLM-Sieve-UP significantly outperform the three state-of-the-art baselines—LASER, SliceGPT, and LLMPruner—all of which prune fewer than 5% of parameters. The strong performance of LLM-Sieve-UP suggests that jointly considering both the input and weight matrix subspaces enables the discovery of more effective task-specific projections. Furthermore, differentiated pruning via the Genetic Algorithm (GA) yields even greater parameter reduction by selectively pruning matrices that are less critical to downstream task performance.

5.3 Does Pruning Generalize to New Datasets of the Same Task?

As seen in Table 1, LLM-Sieve generalizes well across datasets in the same task domain for Gen RAG-II (no loss) and Sentiment-II ($\approx 7\%$ loss). However, performance drops significantly in Med RAG-II. We found that this stems from a mismatch in output format: Med RAG-I requires True/False answers with rationale, whereas Med RAG-II involves multiple-choice selection. This suggests that task-specific pruning generalizes well when output structures are aligned; diverging formats may limit transferability.

Table 1: Generalization of LLM-Sieve-GA across datasets for the same task (LLaMA-3.1-8B).

Task	Test Dataset	Uncompressed Accuracy [%]	LLM-Sieve-GA Accuracy [%]
General RAG	Gen RAG-II	66.8	67.0
Medical Q&A	Med RAG-II	70.5	35.0
Sentiment Analysis	Sentiment-II	91.2	83.5

5.4 Can LoRA Fine-Tuning Improve Accuracy of Pruned Models?

LoRA fine-tuning [4] is commonly used to specialize LLMs for specific tasks. While it often improves accuracy, we find that *over-reliance on LoRA can compromise generalization across datasets within the same task domain*. Figure 8 shows the effect of LoRA when fine-tuned on the same dataset used for calibration. As seen from the figure, LLM-Sieve-GA’s performance improves by the use of LoRA similar to the improvement in the original model for all three tasks. In contrast, methods like LASER and LLM-Pruner, which show near-zero accuracy before LoRA, jump to 50–90% accuracy after LoRA fine-tuning—highlighting their strong dependence on post-pruning adaptation. As we discuss next, however, this over-reliance undermines dataset generalization.

As shown in Figure 9, when pruned models are evaluated on unseen datasets within the same task category, LLM-Sieve shows minimal benefit from LoRA, yet its accuracy remains close to that of the original model on Gen RAG-II and Sentiment-II. This aligns with expectations, as LoRA fine-tuning tends to specialize models to the calibration dataset. Interestingly, on Med RAG-II, LoRA actually reduces LLM-Sieve’s accuracy. Upon inspection, we found that Med RAG-I uses true/false answers, while Med RAG-II requires multiple-choice responses—yet LoRA-tuned models continued producing

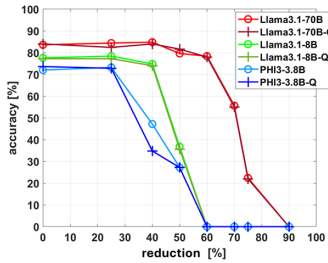


Figure 10: Accuracy vs. pruning % with and without 8-bit quantization.

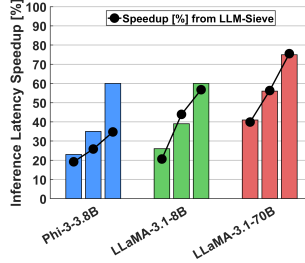


Figure 11: Reduction in parameters vis-a-vis reduction in inference time (speedup for LLM-Sieve).

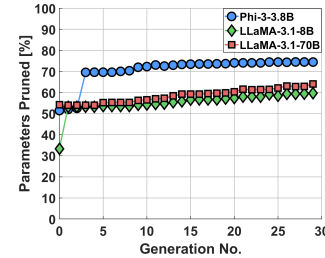


Figure 12: How genetic algorithm parameter reduction evolves across generations.

true/false outputs despite prompt instructions. In contrast, methods like LASER and LLM-Pruner, which depend heavily on LoRA for recovery, fail to match LLM-Sieve’s task-level generalization.

5.5 How much does pruning reduce inference latency?

Figure 11 shows the reduction in inference latency (wall-clock time) across three models and pruning levels, using the CUTLASS [30] library to accelerate tensor operations. All pruned matrix dimensions were constrained to powers of two. We observe that latency speedup scales approximately linearly with the fraction of parameters removed.

5.6 How does quantization affect LLM-Sieve?

Quantization reduces memory and latency by encoding weights in lower-precision formats such as 8-bit integers. As shown in Figure 10, accuracy vs. model size curves for Gen RAG-I using LLM-Sieve-GA (with and without quantization) on Phi-3-3.8B, LLaMA-3.1-8B, and LLaMA-3.1-70B show a plateau followed by a sharp accuracy drop—indicating that many parameters are not task-critical. Notably, the quantized models (marked with “-Q”) closely track the unquantized ones, suggesting that quantization can be applied after pruning to halve memory costs with minimal accuracy loss.

5.7 Running time for LLM-Sieve

Running LLM-Sieve incurs a one-time cost comparable to LoRA fine-tuning. As shown in Table 2, pruning itself requires 1–36 GPU hours depending on the model. The search for pruning factors is more expensive, as it resembles hyperparameter tuning and involves multiple pruning iterations. Uniform pruning via binary search (Sieve-UP) is more efficient, typically converging within 2–4 steps. As shown in Figure 12, the Genetic Algorithm (GA) used in differentiated pruning converges within 10–15 generations, with total cost ranging from 144–900 GPU hours.

Table 2: GPU Hours Spent

Model	Pruning	Sieve-UP	Sieve-GA
Phi-3-3.8B	2	5	144
LLaMA-3.1-8B	3	8	270
LLaMA-3.1-70B	35	85	891

6 Conclusion, Limitations & Future Work

We introduced LLM-Sieve, a task-specific pruning framework that significantly reduces LLM size while preserving accuracy. By combining joint low-rank projections with a Genetic Algorithm for differentiated pruning, LLM-Sieve enables fine-grained compression tailored to task structure. It outperforms prior methods across models and tasks, and remains compatible with LoRA fine-tuning and quantization—supporting a practical pipeline for efficient, task-adapted LLMs. A key limitation is that LLM-Sieve retains the full model architecture, including layer count, which caps compression potential. In contrast, distillation can yield much smaller models (e.g., LLaMA-8B from LLaMA-70B) but at significantly higher cost. Currently, pruning is done per-matrix to avoid backpropagation through non-linearities, and the Genetic Algorithm, while effective, may be replaced by faster pruning factor search methods. We believe LLM-Sieve also opens avenues for interpretability by helping researchers identify which components are essential for each task—potentially shedding light on how knowledge and reasoning are organized within LLMs.

References

- [1] Xunyu Zhu, Jian Li, Yong Liu, Can Ma, and Weiping Wang. A survey on model compression for large language models. *Transactions of the Association for Computational Linguistics*, 12: 1556–1577, 2024.
- [2] Saleh Ashkboos, Maximilian L Croci, Marcelo Gennari do Nascimento, Torsten Hoefer, and James Hensman. Slicept: Compress large language models by deleting rows and columns. *arXiv preprint arXiv:2401.15024*, 2024.
- [3] Pratyusha Sharma, Jordan T Ash, and Dipendra Misra. The truth is in there: Improving reasoning in language models with layer-selective rank reduction. *arXiv preprint arXiv:2312.13558*, 2023.
- [4] Edward J Hu, Yelong Shen, Phillip Wallis, Zeyuan Allen-Zhu, Yanzhi Li, Shean Wang, Lu Wang, and Weizhu Chen. Lora: Low-rank adaptation of large language models. *arXiv preprint arXiv:2106.09685*, 2021.
- [5] Ofir Zafir, Ariel Larey, Guy Boudoukh, Haihao Shen, and Moshe Wasserblat. Prune once for all: Sparse pre-trained language models. *arXiv preprint arXiv:2111.05754*, 2021.
- [6] Jonathan Frankle and Michael Carbin. The lottery ticket hypothesis: Finding sparse, trainable neural networks. *arXiv preprint arXiv:1803.03635*, 2018.
- [7] Elias Frantar and Dan Alistarh. Sparsegpt: Massive language models can be accurately pruned in one-shot. In *International Conference on Machine Learning*, pages 10323–10337. PMLR, 2023.
- [8] Mingjie Sun, Zhuang Liu, Anna Bair, and J Zico Kolter. A simple and effective pruning approach for large language models. *arXiv preprint arXiv:2306.11695*, 2023.
- [9] Xinyin Ma, Gongfan Fang, and Xinchao Wang. Llm-pruner: On the structural pruning of large language models. *Advances in neural information processing systems*, 36:21702–21720, 2023.
- [10] Matan Ben Noach and Yoav Goldberg. Compressing pre-trained language models by matrix decomposition. In *Proceedings of the 1st Conference of the Asia-Pacific Chapter of the Association for Computational Linguistics and the 10th International Joint Conference on Natural Language Processing*, pages 884–889, 2020.
- [11] Elias Frantar, Saleh Ashkboos, Torsten Hoefer, and Dan Alistarh. Gptq: Accurate post-training quantization for generative pre-trained transformers. *arXiv preprint arXiv:2210.17323*, 2022.
- [12] Guangxuan Xiao, Ji Lin, Mickael Seznec, Hao Wu, Julien Demouth, and Song Han. Smoothquant: Accurate and efficient post-training quantization for large language models. In *International Conference on Machine Learning*, pages 38087–38099. PMLR, 2023.
- [13] Saleh Ashkboos, Amirkeivan Mohtashami, Maximilian Croci, Bo Li, Pashmina Cameron, Martin Jaggi, Dan Alistarh, Torsten Hoefer, and James Hensman. Quarot: Outlier-free 4-bit inference in rotated llms. *Advances in Neural Information Processing Systems*, 37:100213–100240, 2024.
- [14] Zechun Liu, Changsheng Zhao, Igor Fedorov, Bilge Soran, Dhruv Choudhary, Raghuraman Krishnamoorthi, Vikas Chandra, Yuandong Tian, and Tijmen Blankevoort. Spinqant: Llm quantization with learned rotations. *arXiv preprint arXiv:2405.16406*, 2024.
- [15] Amir Gholami, Sehoon Kim, Zhen Dong, Zhewei Yao, Michael W Mahoney, and Kurt Keutzer. A survey of quantization methods for efficient neural network inference. In *Low-Power Computer Vision*, pages 291–326. Chapman and Hall/CRC, 2022.
- [16] Torsten Hoefer, Dan Alistarh, Tal Ben-Nun, Nikoli Dryden, and Alexandra Peste. Sparsity in deep learning: Pruning and growth for efficient inference and training in neural networks. *Journal of Machine Learning Research*, 22(241):1–124, 2021.
- [17] Geoffrey Hinton. Distilling the knowledge in a neural network. *arXiv preprint arXiv:1503.02531*, 2015.

- [18] A Vaswani. Attention is all you need. *Advances in Neural Information Processing Systems*, 2017.
- [19] Jimmy Lei Ba. Layer normalization. *arXiv preprint arXiv:1607.06450*, 2016.
- [20] Biao Zhang and Rico Sennrich. Root mean square layer normalization. *Advances in Neural Information Processing Systems*, 32, 2019.
- [21] Zhilin Yang, Peng Qi, Saizheng Zhang, Yoshua Bengio, William W Cohen, Ruslan Salakhutdinov, and Christopher D Manning. Hotpotqa: A dataset for diverse, explainable multi-hop question answering. *arXiv preprint arXiv:1809.09600*, 2018.
- [22] Natural quesetions - short. <https://huggingface.co/datasets/cjloving/natural-questions-short>. [Accessed 16-05-2025].
- [23] Qiao Jin, Bhuwan Dhingra, Zhengping Liu, William W Cohen, and Xinghua Lu. Pubmedqa: A dataset for biomedical research question answering. *arXiv preprint arXiv:1909.06146*, 2019.
- [24] Medmcqa. <https://huggingface.co/datasets/openlifescienceai/medmcqa>. [Accessed 16-05-2025].
- [25] Andrew Maas, Raymond E Daly, Peter T Pham, Dan Huang, Andrew Y Ng, and Christopher Potts. Learning word vectors for sentiment analysis. In *Proceedings of the 49th annual meeting of the association for computational linguistics: Human language technologies*, pages 142–150, 2011.
- [26] Stanford sentiment treebank. <https://huggingface.co/datasets/stanfordnlp/sst>. [Accessed 16-05-2025].
- [27] Lianmin Zheng, Wei-Lin Chiang, Ying Sheng, Siyuan Zhuang, Zhanghao Wu, Yonghao Zhuang, Zi Lin, Zhuohan Li, Dacheng Li, Eric Xing, et al. Judging llm-as-a-judge with mt-bench and chatbot arena. *Advances in Neural Information Processing Systems*, 36:46595–46623, 2023.
- [28] C. J. Van Rijsbergen. *Information Retrieval*. Butterworth-Heinemann, 2nd edition, 1979.
- [29] Woosuk Kwon, Zhuohan Li, Siyuan Zhuang, Ying Sheng, Lianmin Zheng, Cody Hao Yu, Joseph Gonzalez, Hao Zhang, and Ion Stoica. Efficient memory management for large language model serving with pagedattention. In *Proceedings of the 29th Symposium on Operating Systems Principles*, pages 611–626, 2023.
- [30] CUTLASS. <https://docs.nvidia.com/cutlass/>. [Accessed 16-05-2025].

A Appendix

A.1 Calibration Dataset Sensitivity.

To assess the impact of calibration dataset size, we ran a sensitivity analysis on Phi-3-mini for all our tasks using LLM-Sieve configured with uniform pruning. As seen in Fig. 13, we observe that accuracy plateaus after approximately 150K tokens. Based on this, we use a fixed calibration set of 200K tokens for all our pruning experiments.

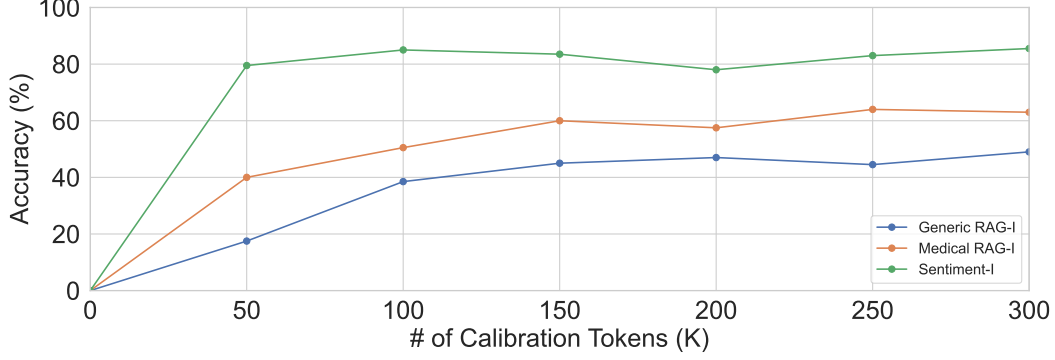


Figure 13: Sensitivity to different calibration dataset sizes for Phi-3-mini. The accuracy benefits start to plateau after 150K tokens.

A.2 Compressibility of different matrix types.

In our genetic algorithm (GA) hyperparameter search, we observed that different matrix types within the feedforward and attention components exhibit varying degrees of compressibility. Figure 14 presents the average fraction of parameters retained per matrix type, averaged across all layers, for the best-performing GA configuration. These results cover all model and dataset combinations. We find that for LLaMA-3.1 8B and 70B, feedforward matrices such as W_1 and W_2 are generally more compressible than their attention counterparts. This pattern is not observed in Phi-3-mini.

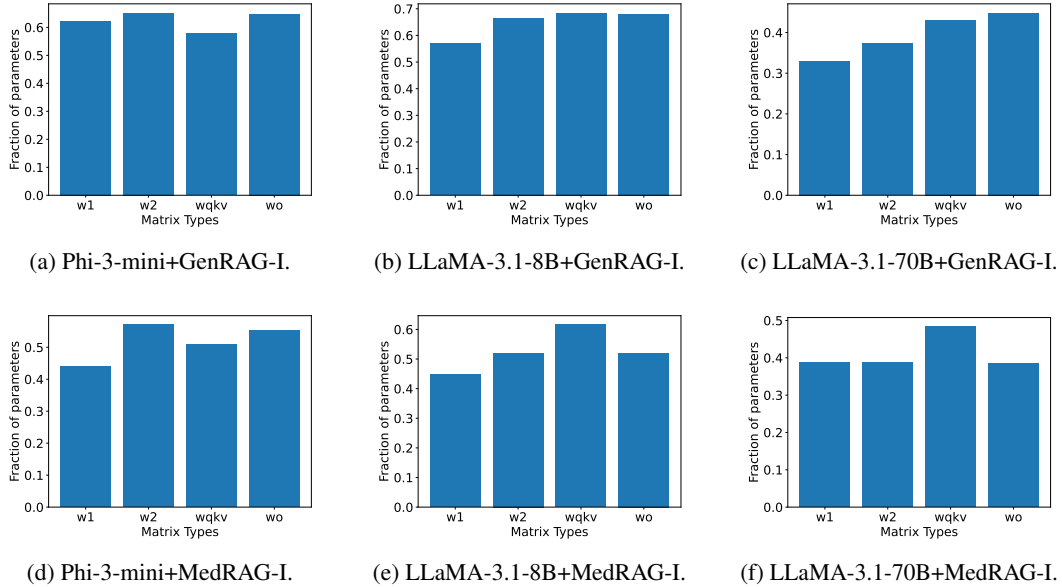
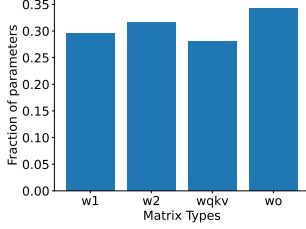
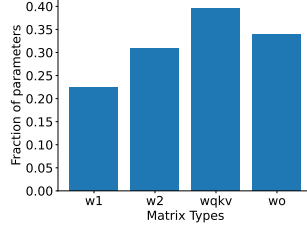


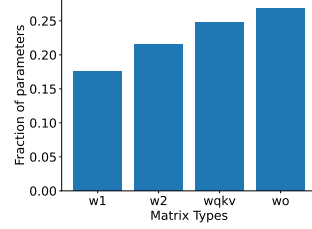
Figure 14: Fraction of remaining parameters for each matrix type found using our Genetic Algorithm search (lower values = higher compression).



(g) Phi-3-mini+Sentiment-I.



(h) LLaMA-3.1-8B+Sentiment-I.

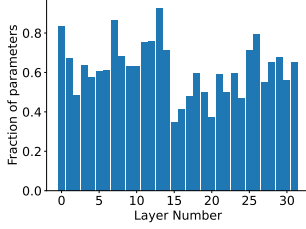


(i) LLaMA-3.1-70B+Sentiment-I.

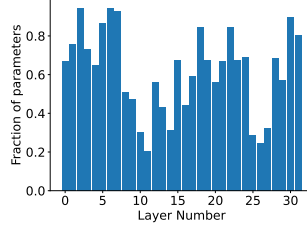
Figure 14: (Continued)

A.3 Compressibility of different Layers.

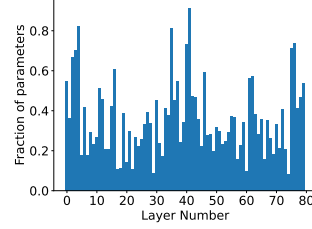
Figure 15 presents the average fraction of parameters retained per layer. For larger models such as LLaMA-3.1-70B, we observe a trend where the second half of layers tends to be significantly more compressible than the first half, with the exception of the final few layers. This pattern is especially pronounced in narrower, more specialized tasks like sentiment analysis (Fig. 15i). In contrast, for smaller models such as Phi-3-mini and LLaMA-3.1-8B, no consistent compressibility trend emerges across the different layers.



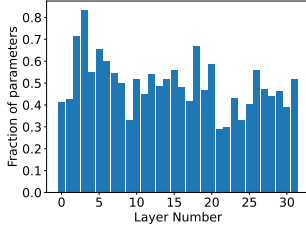
(a) Phi-3-mini+GenRAG-I.



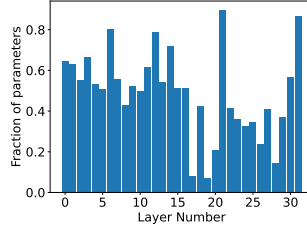
(b) LLaMA-3.1-8B + GenRAG-I.



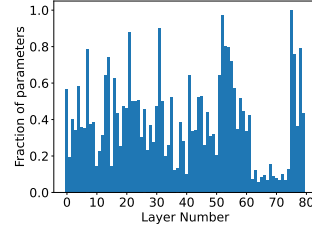
(c) LLaMA-3.1-70B+GenRAG-I.



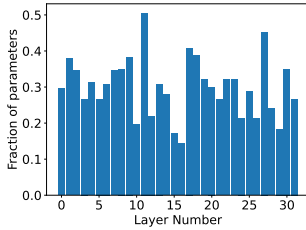
(d) Phi-3-mini+MedRAG-I.



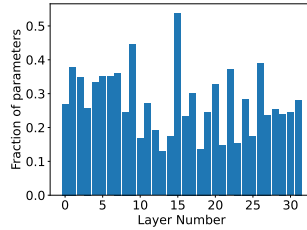
(e) LLaMA-3.1-8B+MedRAG-I.



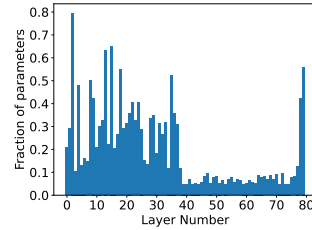
(f) LLaMA-3.1-70B+MedRAG-I.



(g) Phi-3-mini+Sentiment-I.



(h) LLaMA-3.1-8B+Sentiment-I.



(i) LLaMA-3.1-70B+Sentiment-I.

Figure 15: Fraction of remaining parameters for each layer in the model after conducting a Genetic Algorithm search (lower numbers imply higher compression).

A.4 Presence of Bottleneck Matrices.

We perform a cross-population analysis of the top-performing individuals—defined as those within 20% of the best recorded fitness—during our genetic algorithm search. For each matrix in every layer, we compute the probability that it remains unpruned (i.e., receives zero compression) across these individuals. As seen in Fig. 16, for LLaMA-3.1-70B, we consistently find matrices that are never pruned across all top individuals (highlighted in red), indicating that pruning these matrices leads to significant performance degradation. We refer to these as *bottleneck matrices*. This phenomenon suggests that larger models tend to hyperspecialize certain matrices for critical sub-tasks and exhibit limited tolerance to pruning in those areas.

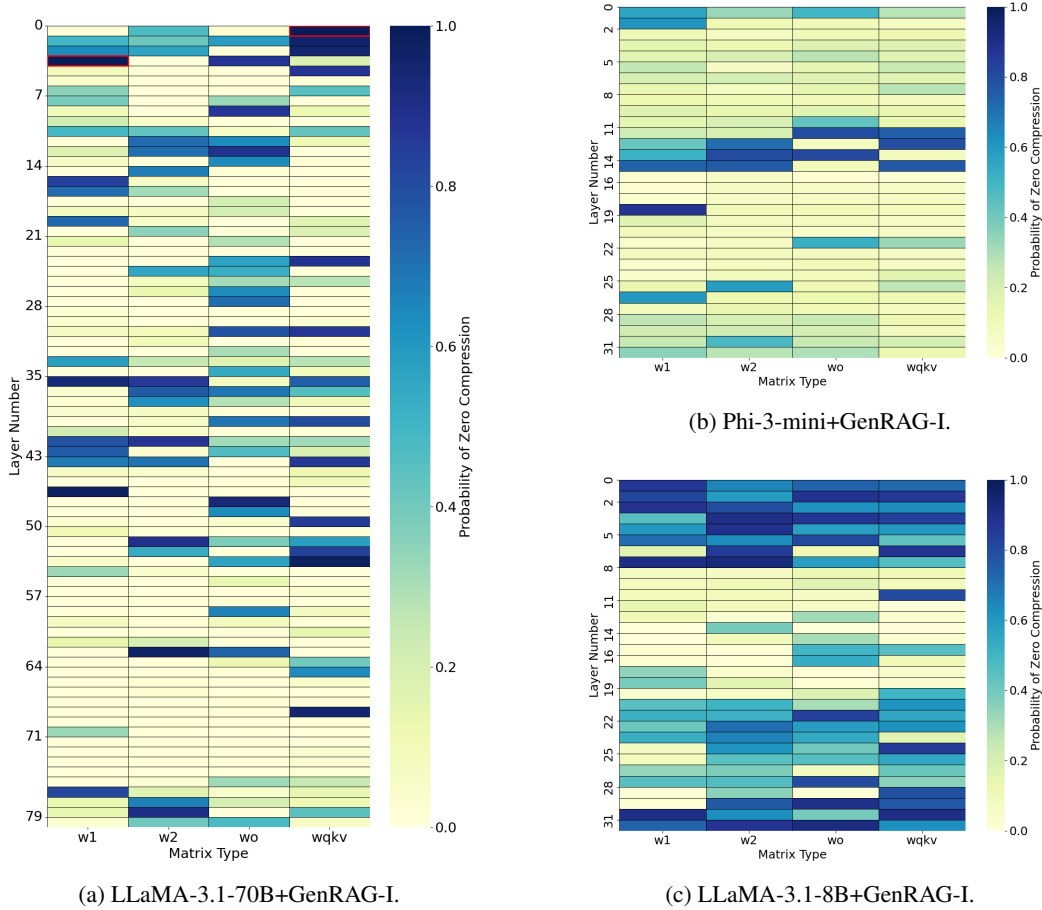
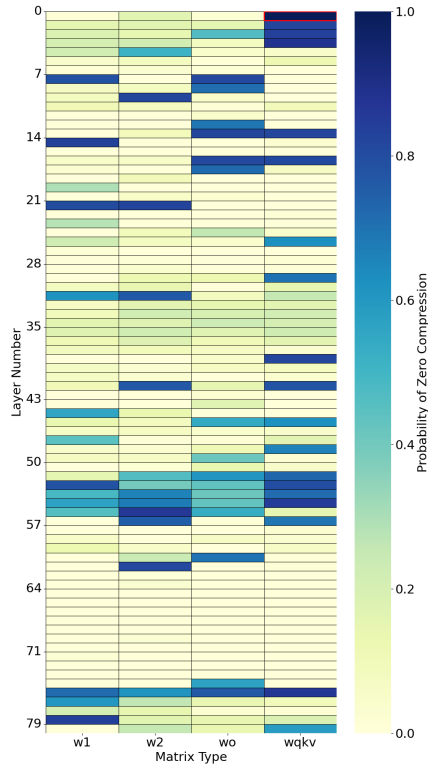
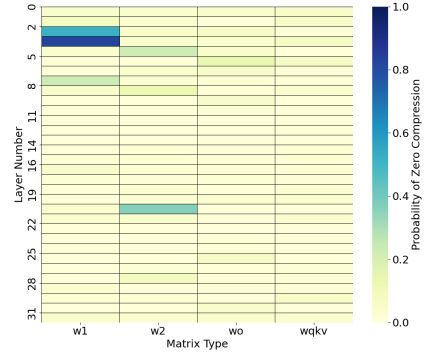


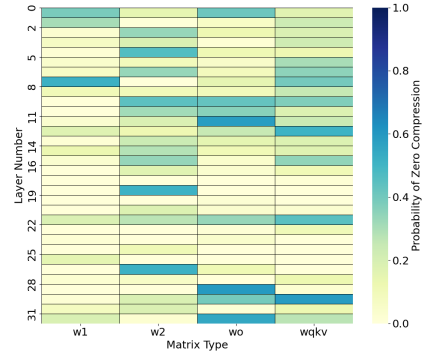
Figure 16: Heat map showing the bottleneck matrices during GA for different models/datasets. Boxes highlighted in red indicate that the matrix is unprunable (i.e., pruning results in significant loss).



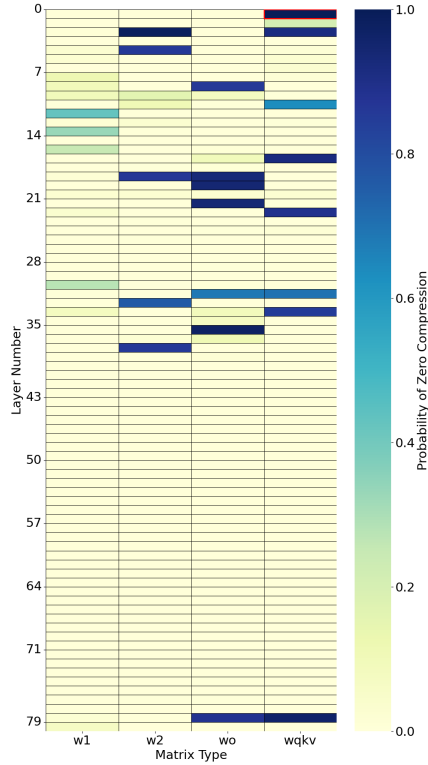
(d) LLaMA-3.1-70B+MedRAG-I.



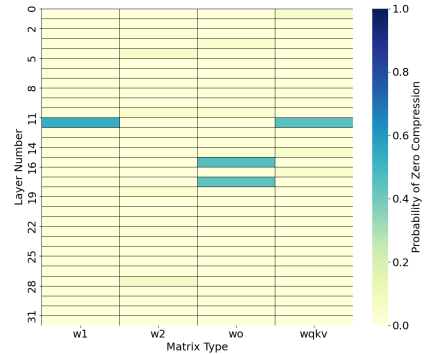
(e) Phi-3-mini+MedRAG-I.



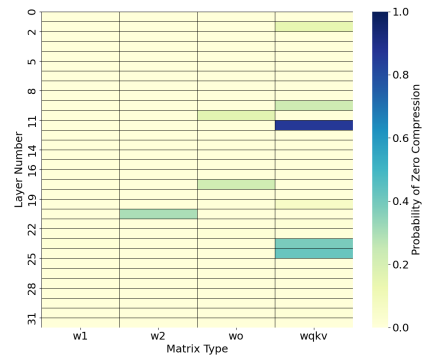
(f) LLaMA-3.1-8B+MedRAG-I.



(g) LLaMA-3.1-70B+Sentiment-I.



(h) Phi-3-mini+Sentiment-I.



(i) LLaMA-3.1-8B+Sentiment-I.

Figure 16: (Continued)